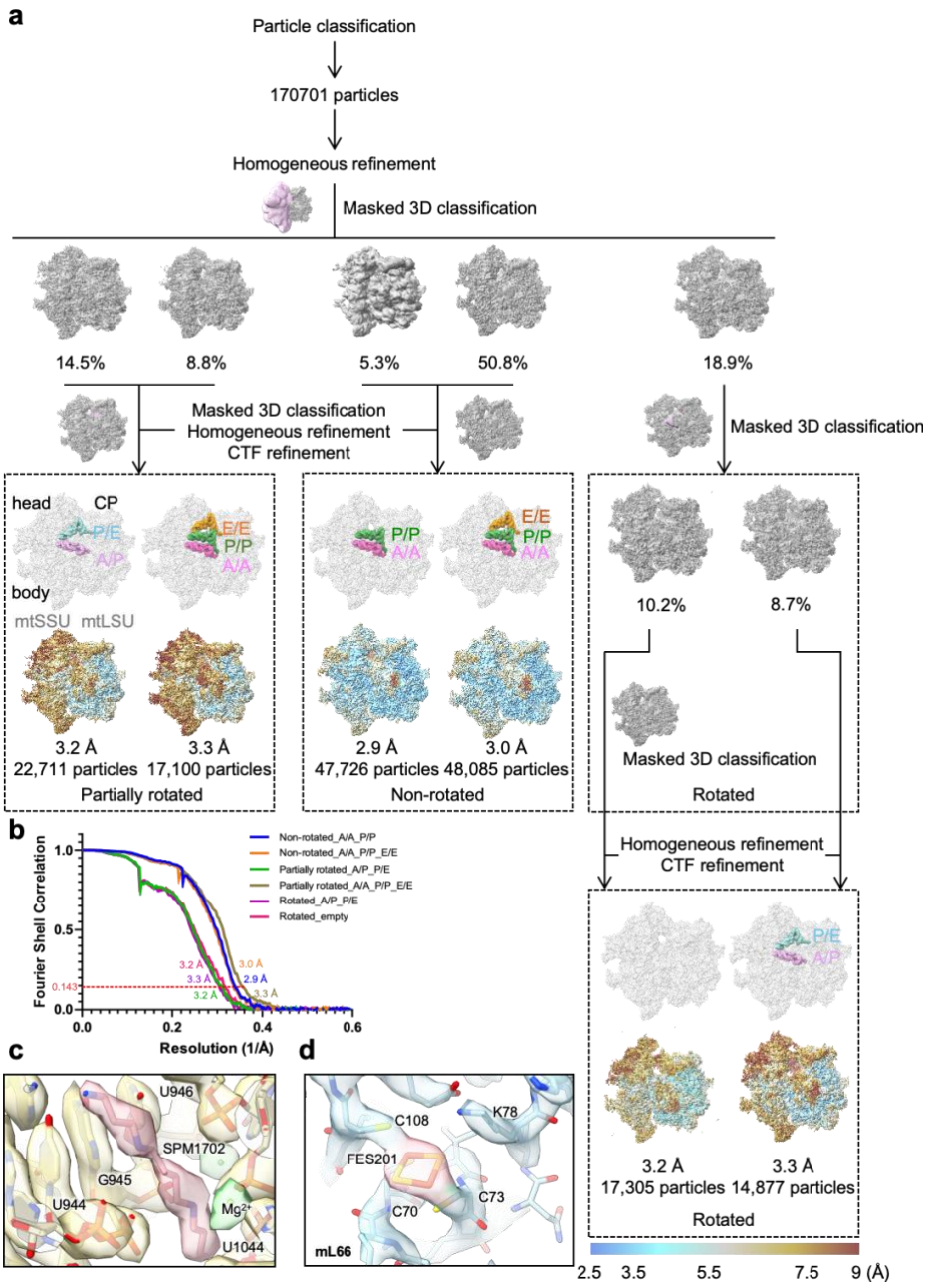

Supplementary Fig. 1| Cryo-EM data processing of neomycin-treated mitoribosomes. **a** Cryo-EM data processing workflow of mitoribosomes incubated with 50 μM neomycin. Overall structures of mitoribosomes with bound tRNAs and cofactors, along with local resolution estimation results with the resolution scale (Å) are shown. **b** Fourier shell correlation (FSC) curves for the reported maps, indicating overall resolution at FSC=0.143. **c-d** cryo-EM density for representative cofactors from the same map as Fig. 1 are displayed: SPM1702 **(c)** and FES201 **(d)** bound to the non-rotated mitoribosome with A/A and P/P site tRNA (overall resolution=2.9 Å, σ=0.90).

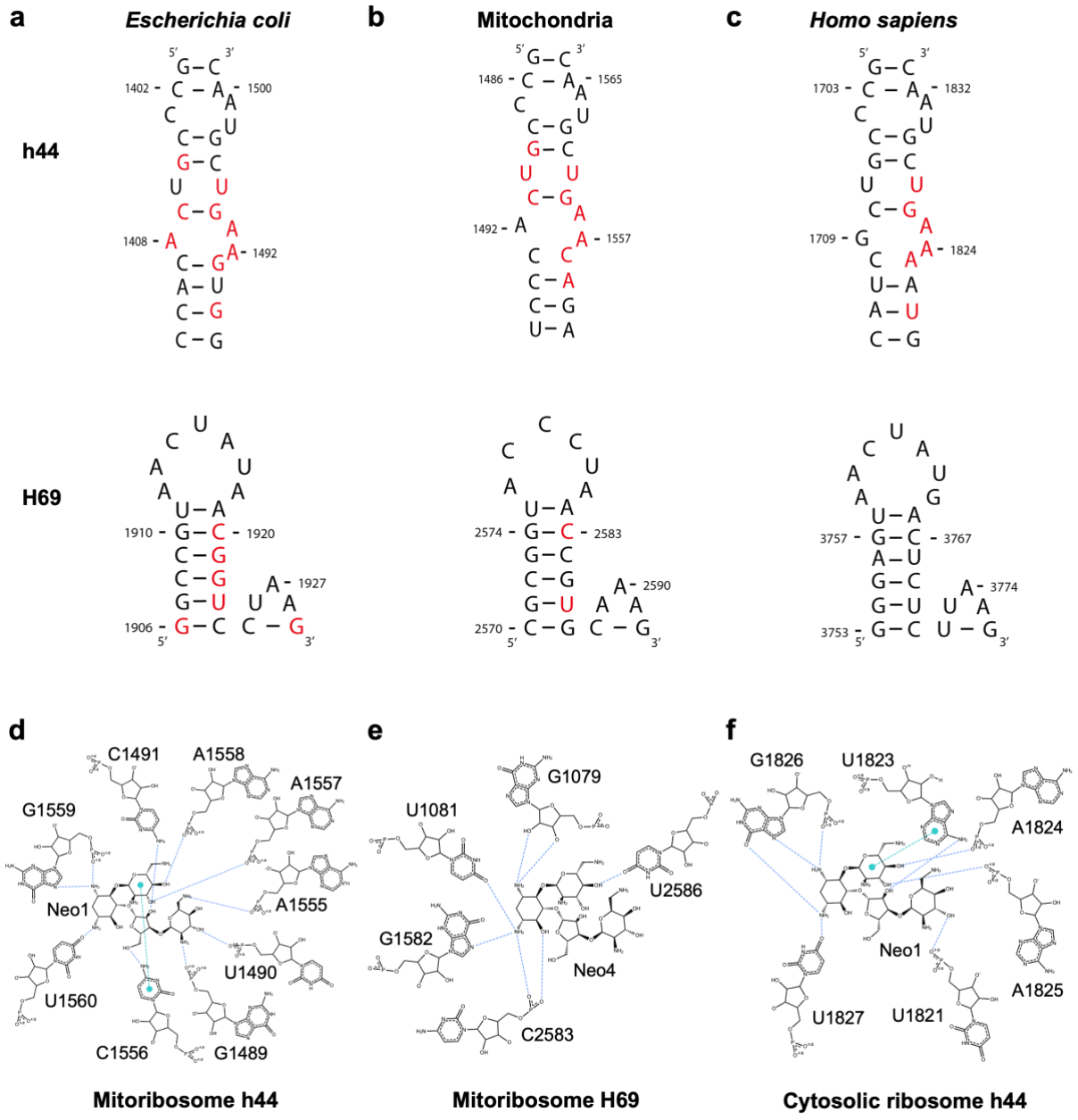

Supplementary Fig. 2| Comparative analysis of h44 and H69, and neomycin binding. **a-c** Secondary structures of h44 and H69 from *Escherichia coli* **(a)**, mitochondria **(b),** and *Homo sapiens* **(c)** ribosomes. **d-f** Schematic representation of h44 and H69 interactions with neomycin.

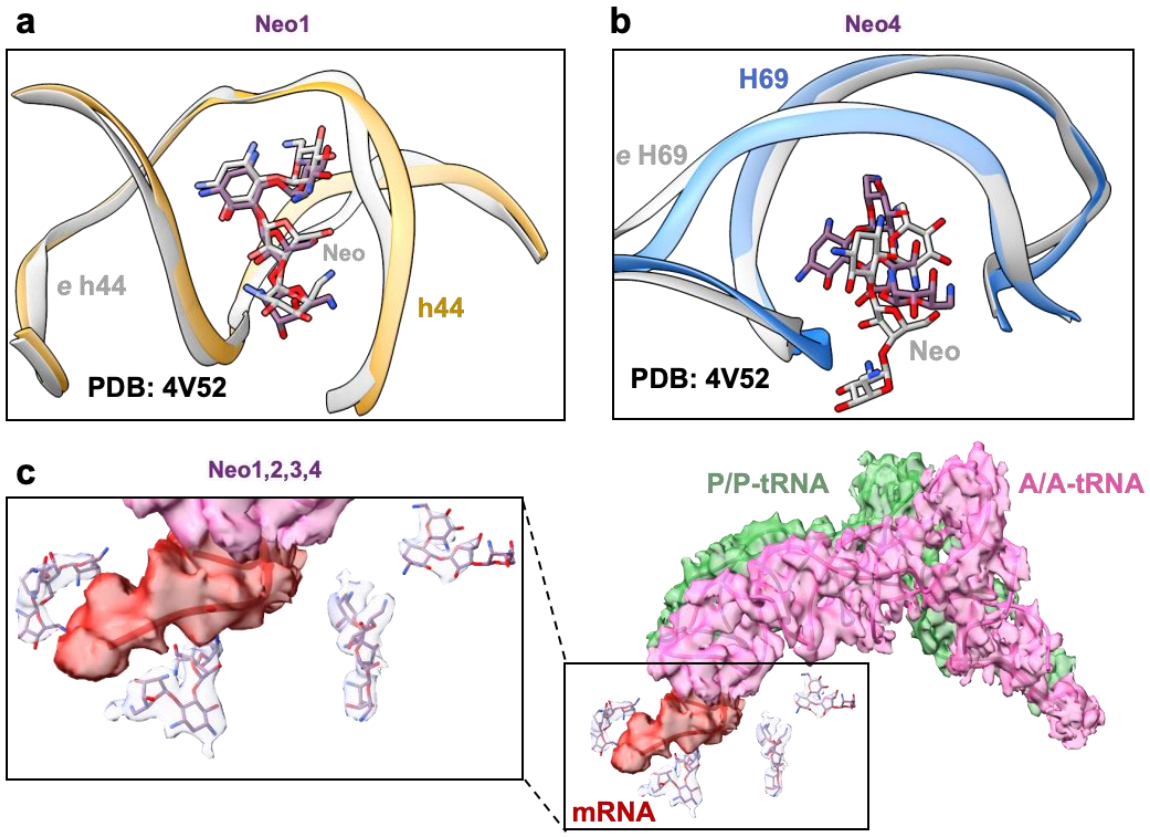

Supplementary Fig. 3| Structural analysis of neomycin's binding to mitoribosome's decoding center. a-b Superimposition of neomycin binding pockets within h44 **(a)** and H69 **(b)** with the bacterial ribosome (PDB: 4V52[9]). **c** Overview of the mRNA decoding center with bound neomycin molecules. A zoomed inset highlights the bound neomycin molecules.

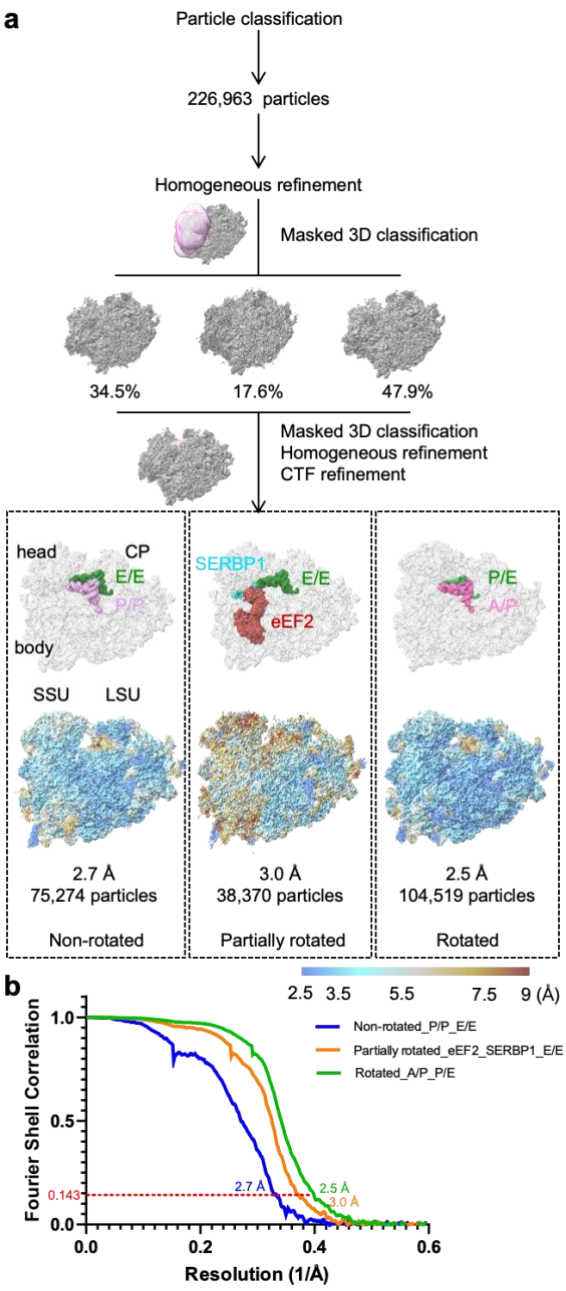

Supplementary Fig. 4| Cryo-EM data processing of neomycin-treated cytosolic ribosomes. **a** Cryo-EM data processing workflow of cytosolic ribosomes incubated with 50 μM neomycin. Overall structures of cytosolic ribosomes with different bound tRNAs and cofactors, along with local resolution estimation results with the resolution scale in Å are shown. **b** FSC curves calculated for the reported maps, indicating an overall resolution at FSC = 0.143.

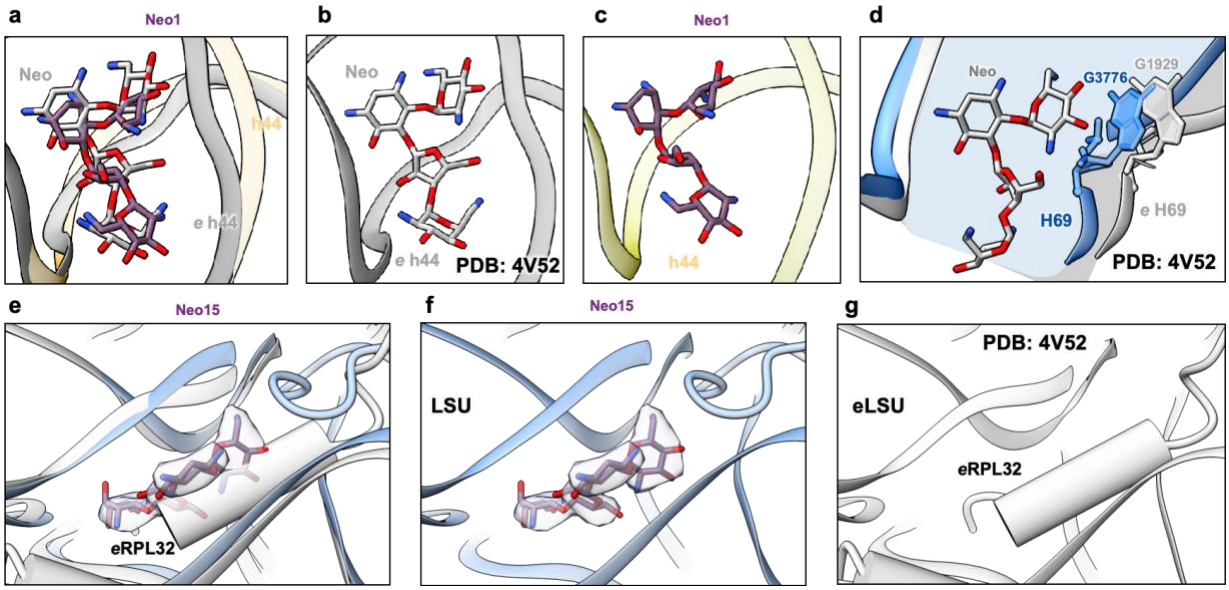

Supplementary Fig. 5| Novel and conserved binding sites of neomycin on the cytosolic ribosome. a-c Neomycin (Neo1) binding to a conserved pocket within h44. **a** Superimposition of the neomycin-bound h44 from this study (yellow) and bacterial ribosome (PDB: 4V52[9], grey). **b** Neomycin molecules bound to the bacterial ribosome**. c** Neomycin molecules bound to human cytosolic ribosome. **d** Superimposition of H69 from this study (blue) and neomycin-bound H69 (grey) from the bacterial ribosome (PDB: 4V52[9]). Potential steric clashes are highlighted, with contributing nucleotides shown as sticks. The area size of the H69 pocket is indicated in blue (human) and grey (bacteria). **e-g** Interaction of neomycin (Neo15) with a novel cytosolic ribosomal pocket. **e** Superimposition of the neomycin-bound pocket from this study (blue) and bacterial ribosome (PDB: 4V52[9], grey). This neomycin binding pocket is typically occupied by RPL32 in the bacterial ribosome. **f** Neo15 is shown interacting with this novel cytosolic ribosomal pocket. **g** The corresponding pocket is occupied by RPL32 in the bacterial ribosome.

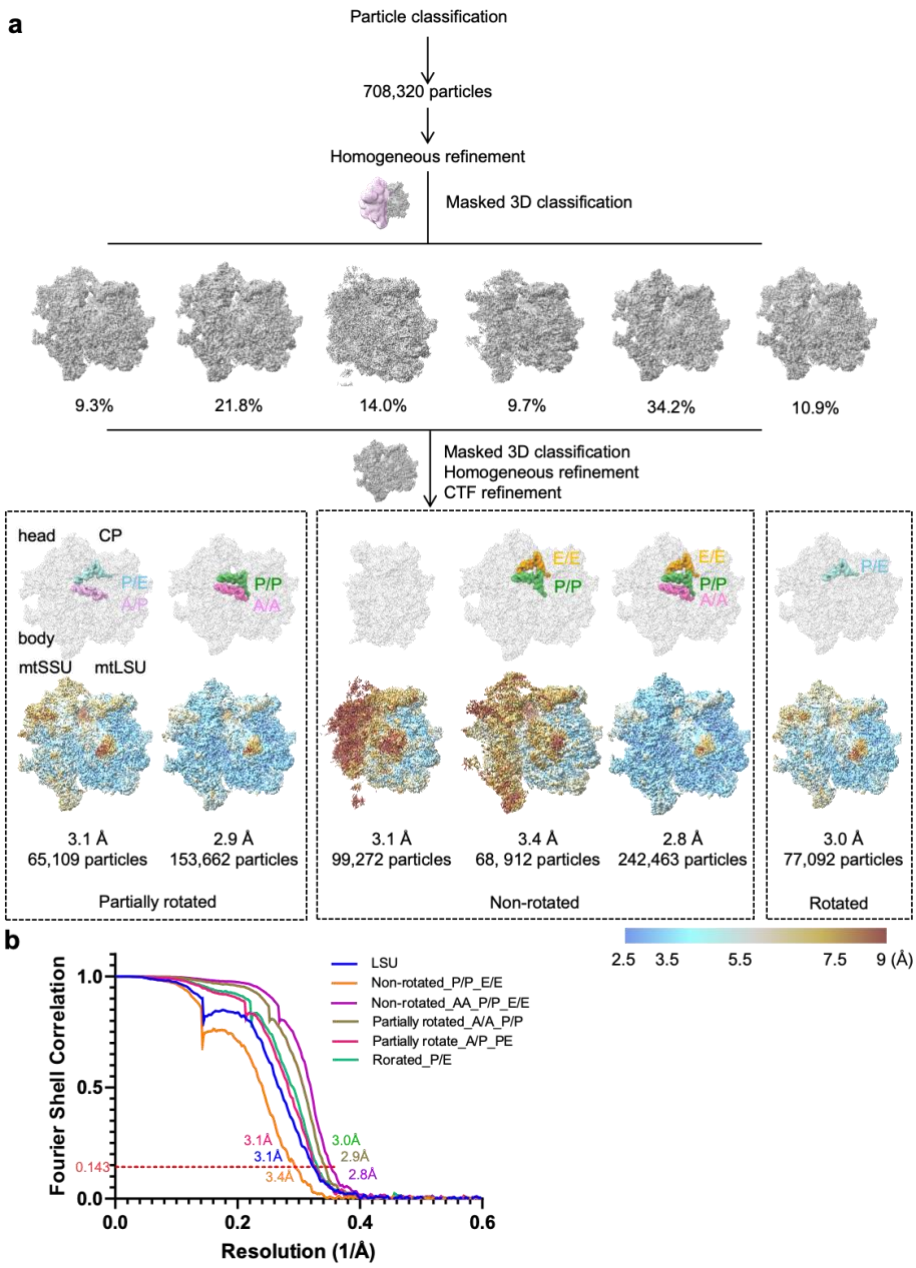

Supplementary Fig. 6| Cryo-EM data processing of mitoribosomes from neomycin-treated cells. a Cryo-EM data processing workflow for native mitoribosomes isolated from 1 mM neomycin-treated cells. Overall structures of mitoribosomes with bound tRNAs and cofactors, along with local resolution estimation results with resolution scale in Å are shown. **b** FSC curves calculated for the reported maps, indicating an overall resolution at FSC = 0.143.

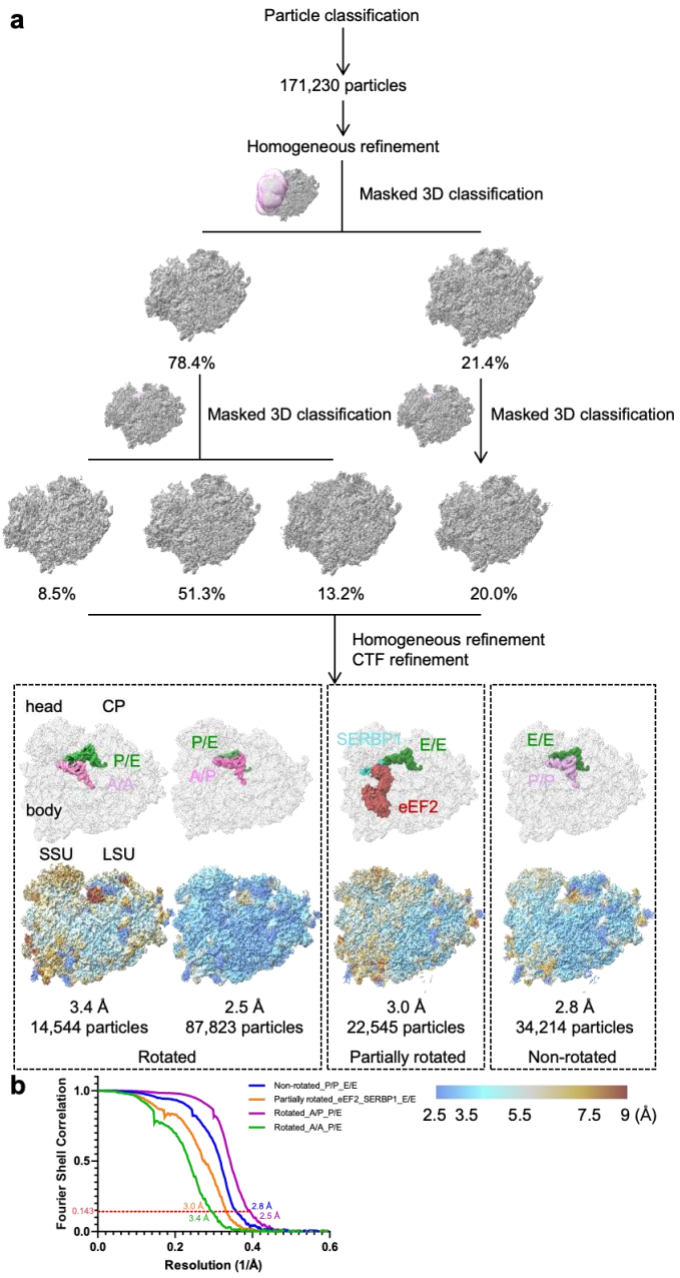

Supplementary Fig. 7| Cryo-EM data processing of cytosolic ribosomes from neomycin-treated cells. **a** Cryo-EM data processing workflow for native cytosolic ribosomes isolated from 1 mM neomycin-treated cells. Overall structures of cytosolic cytosolic ribosomes with different bound tRNAs and cofactors, along with local resolution estimation results with resolution scale in Å are shown. **b** FSC curves calculated for the reported maps, indicating an overall resolution at FSC = 0.143.

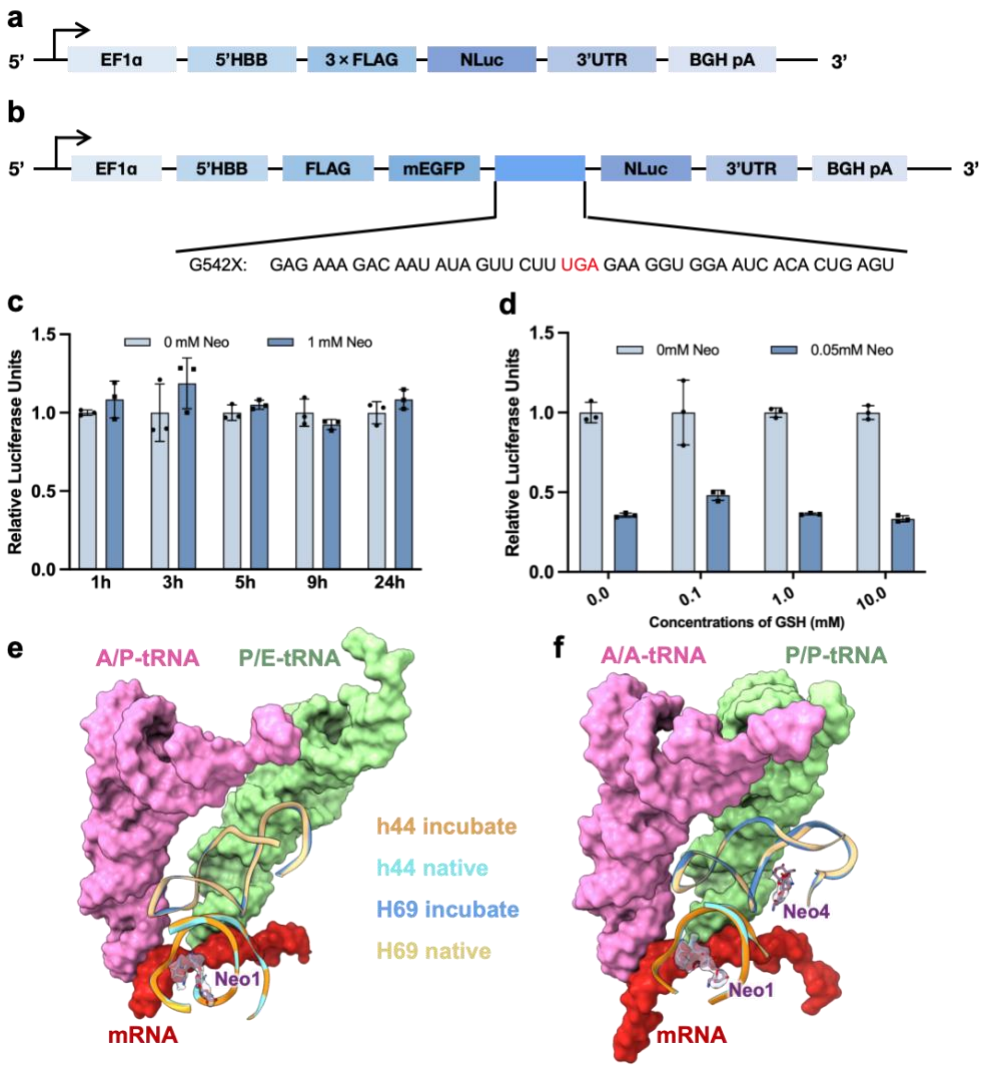

Supplementary Fig. 8| *In vivo* translation assays and structural analysis of the decoding center. a Schematic representation of the NLuc (**a**) and CFTR (G542X) (**b**) lentiviral constructs used to create stable cell lines. **c** Luciferase reporter assays using the NLuc cell line at various time points following treatment with different concentrations of neomycin. **d** *In vitro* translation assays with luciferase reporters in response to different concentrations of neomycin and increased concentrations of 0.1, 1 and 10 mM GSH. **e-f** Structure superimposition of decoding centers from the cytosolic ribosome **(e)** and mitoribosome **(f)** undergoing different neomycin treatments.

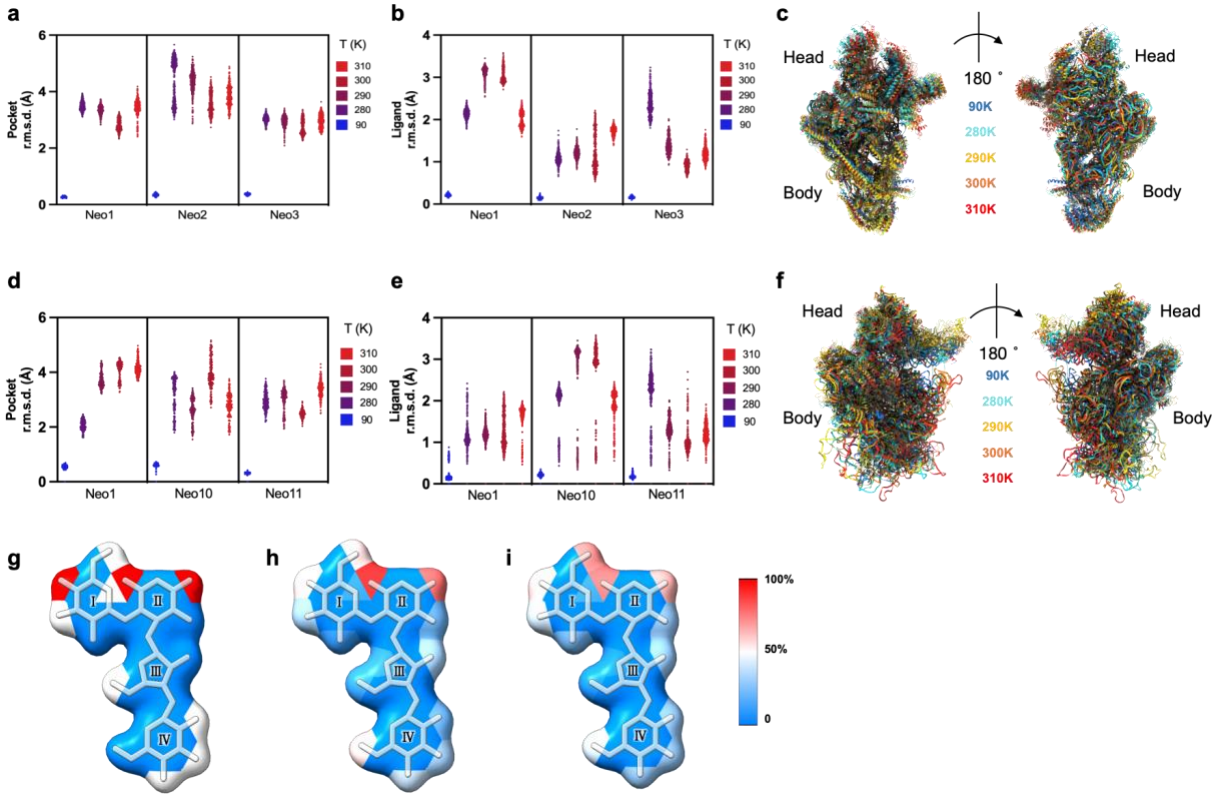

Supplementary Fig. 9| Temperature-dependent MD simulations of neomycin-ribosome interactions and neomycin contact modules. a-b MD simulations depicting the temperature-dependent binding stability of neomycin molecules (Neo1, Neo2, and Neo3) within mtSSU. The RMSD from their initial binding poses of both the binding pockets **(a)** and the neomycin molecules **(b),** across temperatures from 90 K to 310 K. **c** Representative mtSSU structures generated by temperature-dependent MD simulations. **d-e** MD simulations depicting the temperature-dependent binding stability of neomycin molecules (Neo1, Neo10, and Neo11) within SSU. The RMSD from their initial binding poses of both binding pockets **(d)** and their initial binding poses for neomycin molecules **(e)** are shown across temperatures from 90 K to 310 K. **f** Representative SSU structures generated by temperature-dependent MD simulations. **g-i** Interaction frequency of neomycin's moieties with the bacterial ribosome (**g**), mitoribosome (**h**) and cytosolic ribosome (**i**). The chemical structure of neomycin is represented in stick and surface, with contact frequency indicated by color (blue for low frequency, red for high frequency).

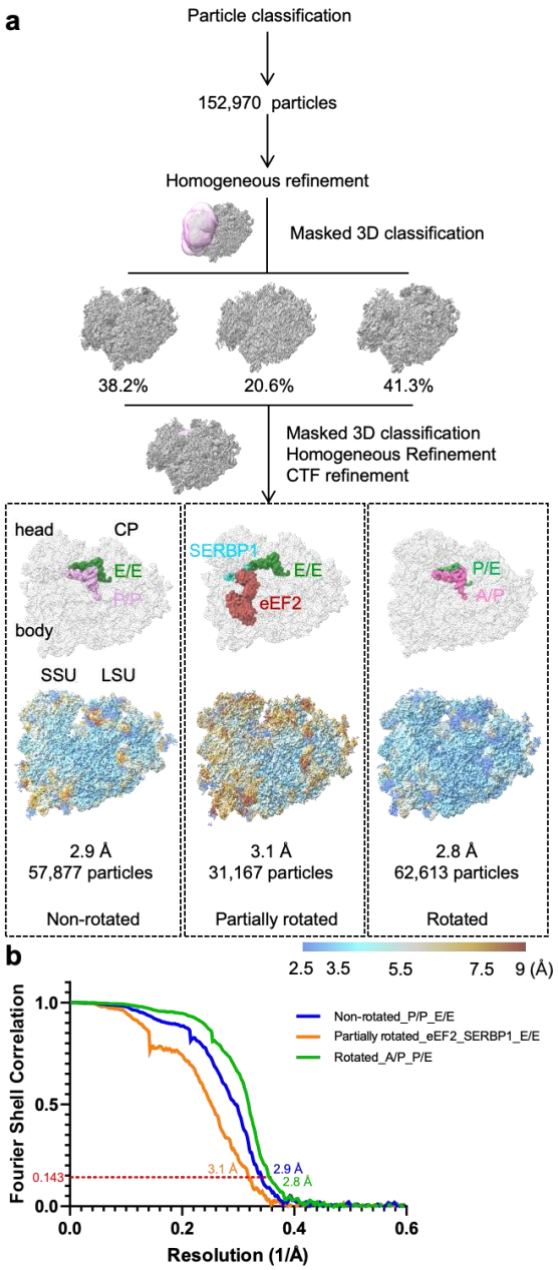

Supplementary Fig. 10| Cryo-EM data processing of mitoribosomes from neomycin-treated cells. a Cryo-EM data processing workflow of native mitoribosomes isolated from 3 mM neomycin-treated cells. Overall structures of mitoribosomes with different bound tRNAs and cofactors, along with local resolution estimation results with resolution scale in Å are shown. **b** FSC curves calculated for the reported maps, indicating an overall resolution at FSC = 0.143.

Supplementary Table. 1| Cryo-EM data collection, processing, model refinement, and validation statistics for mitoribosomes incubated with 50 μM neomycin.

	Mitoribosome, Non-rotated state, A/A-P/P	Mitoribosome, Non-rotated state, A/A-P/P-E/E	Mitoribosome, Partially rotated state, A/A-P/P-E/E	Mitoribosome, Partially rotated state, A/P-P/E	Mitoribosome, Rotated state	Mitoribosome, Rotated state, A/P-P/E
EMDB	65433	65426	65427	65428	65429	65431
PDB	9VXM					
Data collection and processing						
Magnification	96000x	96000x	96000x	96000x	96000x	96000x
Voltage (kV)	300	300	300	300	300	300
Electron exposure (e–/Å^2)	50	50	50	50	50	50
Defocus range (μm)	-1 to -2	-1 to -2	-1 to -2	-1 to -2	-1 to -2	-1 to -2
Pixel size (Å)	0.81	0.81	0.81	0.81	0.81	0.81
Symmetry imposed	*C1*	*C1*	*C1*	*C1*	*C1*	*C1*
Initial particle images (no.)	402,000	402,000	402,000	402,000	402,000	402,000
Final particle images (no.)	47,726	48,085	17,100	22,711	17,305	14,877
Map resolution (Å) FSC threshold	0.143	0.143	0.143	0.143	0.143	0.143
Map resolution range (Å)	2.9	3.0	3.3	3.2	3.2	3.3
Refinement						
Initial model used (PDB code)	7QI5					
Model resolution (Å) FSC threshold	3.1					
Model resolution range (Å)	0.5					
Map sharpening *B* factor (Å^2)	58.6					
Model composition						
Non-hydrogen atoms	176678					
Protein residues	14395					
Ligands	284					
B factors (Å^2)						
Protein	94.20					
Ligand	73.82					
R.m.s. deviations						
Bond lengths (Å)	0.006					
Bond angles (°)	0.966					
Validation						
MolProbity score	2.53					
Clashscore	11.95					
Poor rotamers (%)	4.79					
Ramachandran plot						
Favored (%)	93.68					
Allowed (%)	5.87					
Disallowed (%)	0.45					

Supplementary Table. 2| Neomycin binding pockets in *in vitro* and *in vivo* mitoribosome states. This table details the neomycin molecules bound in different mitoribosome states, including their respective binding pockets and proximal nucleotide information. Asterisks (*) denote the quality of the neomycin density, where the number of asterisks corresponds to the count of discernible organic rings of neomycin in the density map.

Number	Binding pocket	Proximal nucleotide	*In vitro*						*In vivo*					
		State	Mitoribosome, Non-rotated state, A/A-P/P	Mitoribosome, Non-rotated state, A/A-P/P-E/E	Mitoribosome, Partially rotated state, A/A-P/P-E/E	Mitoribosome, Partially rotated state, A/P-P/E	Mitoribosome, Rotated state, E/E	Mitoribosome, Rotated state	mtLSU	Mitoribosome, Non-rotated state, P/P-E/E	Mitoribosome, Non-rotated state, A/A-P/P-E/E	Mitoribosome, Partially rotated state, A/A-P/P	Mitoribosome, Partially rotated state, A/P-P/E	Mitoribosome, Rotated state, P/E
Neo1	h44	12S A1556	****	****	***	****	**	**						
Neo2	h1+h44	12S C1487	****	****	***	***	***	***						
Neo3	h28	12S A1470	****	****	***	****	****	****						
Neo4	H69	16S C2583	***	***										
Neo5	H91+H95	16S G3019	****	****	****		****	****						
Neo6	H35#	16S G1949			***									
Neo7	H33#	16S U2404	****	***		**		****						
Neo8	H73+H72	16S A2707	****	****	***	****	****	****						
Neo9	H39+H37+H75	16S C2116	**	**		**	**	**						

#: rRNA has relatively low conservation.

Supplementary Table. 3| Cryo-EM data collection, processing, model refinement, and validation statistics for cytosolic ribosomes incubated with 50 µM neomycin.

	Cytosolic ribosome, Rotated state, A/P-P/E	Cytosolic ribosome, Partially rotated state, eEF2, SERBP1, E/E	Cytosolic ribosome, Non-rotated state, P/P-E/E
EMDB	65434	65412	65419
PDB	9VXN		
Data collection and processing			
Magnification	96000x	96000x	96000x
Voltage (kV)	300	300	300
Electron exposure (e–/Å^2)	50	50	50
Defocus range (µm)	-1 to -2	-1 to -2	-1 to -2
Pixel size (Å)	0.81	0.81	0.81
Symmetry imposed	*C1*	*C1*	*C1*
Initial particle images (no.)	972,883	972,883	972,883
Final particle images (no.)	104,519	38,370	75,274
Map resolution (Å) FSC threshold	2.5	3.0	2.7
Map resolution range (Å)	0.143	0.143	0.143
Refinement			
Initial model used (PDB code)	8QOI		
Model resolution (Å) FSC threshold	2.8		
Model resolution range (Å)	0.5		
Map sharpening *B*factor (Å^2)	38.8		
Model composition			
Non-hydrogen atoms	217929		
Protein residues	11439		
Ligands	429		
B factors (Å^2)			
Protein	62.89		
Ligand	57.76		
R.m.s. deviations			
Bond lengths (Å)	0.009		
Bond angles (°)	0.956		
Validation			
MolProbity score	2.42		
Clashscore	11.28		
Poor rotamers (%)	4.19		
Ramachandran plot			
Favored (%)	94.51		
Allowed (%)	4.99		
Disallowed (%)	0.51		

Supplementary Table. 4| Neomycin binding pockets in cytosolic ribosome states. This table details the neomycin molecules bound in various cytosolic ribosome states, including their respective binding pockets and proximal nucleotide information. Asterisks (*)denote the quality of the neomycin density, where the number of asterisks corresponds to the count of discernible organic rings of neomycin in the density map.

		State	*In vitro*			*In vivo* (1 mM)				*In vivo* (3 mM)		
Number	Binding pocket	Proximal nucleotide	Cytosolic ribosome, Non-rotated state, P/P-E/E	Cytosolic ribosome, Partially rotated state, eEF2, SERBP1, E/E	Cytosolic ribosome, Rotated state, A/P-P/E	Cytosolic ribosome, Non-rotated state, P/P-E/E	Cytosolic ribosome, Partially rotated state, eEF2, SERBP1, E/E	Cytosolic ribosome, Rotated state, A/A-P/E	Cytosolic ribosome, Rotated state, A/P-P/E	Cytosolic ribosome, Non-rotated state, P/P-E/E	Cytosolic ribosome, Partially rotated state, eEF2, SERBP1, E/E	Cytosolic ribosome, Rotated state, A/P-P/E
Neo1	h44	18S A1825	**	**	***							
Neo10	h28+h37+h40	18S U1343	****		****	****	****		****			
Neo11	h44	18S G1726	****	****	****		**	**	****			
Neo12	H62+H34	28S G2868	****	****	****	****		**	****			
Neo13	H41+H42+H89	28S A1939	****	****	****	****		****	****			
Neo14	H89+H10+H72	28S A2047	****	***	****				***			
Neo15	H24+H26+H2（23S in Prokaryote，28S+5.8S in Eukaryotes）	28S G2358	****	****	****	****	****	****	****	**		**
Neo16	h44	18S G1726	****	****	****		**	**	****			
Neo17	H39+5s rRNA	28S U1861	****	****	****	****	****	****	****			
Neo18	H42	28S C1931	****	****	****	****	****	****	****			
Neo19	H54+H53+L7a	28S G2777	****	**	****			****				
Neo20	H58#	28S G2645	****	***	****	**			**			
Neo21	H91+H95	28S U4481	****	****	****							
Neo22	H58	28S C2683	****	****	****				****			
Neo23	H74	28S C3909		**	****				**			
Neo24	H89+H91+H42+H90	28S A4484			****							
Neo25	H66+h24（The interface of the LSU and SSU）	28S C3696		****	****		****	****	****			

#: rRNA has relatively low conservation

Supplementary Table. 5| Cryo-EM data collection and processing statistics for native mitoribosomes and cytosolic ribosomes isolated from neomycin-treated cells.

Mitoribosomes from 1mM Neo treated cells	mtLSU	Mitoribosome, Non-rotated state, P/P-E/E	Mitoribosome, Non-rotated state, A/A-P/P-E/E	Mitoribosome, Partially rotated state, A/A-P/P	Mitoribosome, Partially rotated state, A/P-P/E	Mitoribosome, Rotated state, P/E
EMDB	65420	65421	65422	65423	65424	65425
Data collection and processing						
Magnification	96000x	96000x	96000x	96000x	96000x	96000x
Voltage (kV)	300	300	300	300	300	300
Electron exposure (e–/Å^2)	50	50	50	50	50	50
Defocus range (μm)	-1 to -2	-1 to -2	-1 to -2	-1 to -2	-1 to -2	-1 to -2
Pixel size (Å)	0.81	0.81	0.81	0.81	0.81	0.81
Symmetry imposed	*C1*	*C1*	*C1*	*C1*	*C1*	*C1*
Initial particle images (no.)	1,043,603	1,043,603	1,043,603	1,043,603	1,043,603	1,043,603
Final particle images (no.)	99,272	68,912	242,463	153,662	65,109	77,092
Map resolution (Å) FSC threshold	3.1	3.4	2.8	2.9	3.1	3.0
Map resolution range (Å)	0.143	0.143	0.143	0.143	0.143	0.143

Cytosolic ribosomes from 1mM Neo treated cells	Cytosolic ribosome, Non-rotated state, P/P-E/E	Cytosolic ribosome, Partially rotated state, eEF2, SERBP1, E/E	Cytosolic ribosome, Rotated state, A/A-P/E	Cytosolic ribosome, Rotated state, A/P-P/E
EMDB	65411	65413	65414	65415
Data collection and processing				
Magnification	96000x	96000x	96000x	96000x
Voltage (kV)	300	300	300	300
Electron exposure (e–/Å^2)	50	50	50	50
Defocus range (μm)	-1 to -2	-1 to -2	-1 to -2	-1 to -2
Pixel size (Å)	0.81	0.81	0.81	0.81
Symmetry imposed	*C1*	*C1*	*C1*	*C1*
Initial particle images (no.)	338,609	338,609	338,609	338,609
Final particle images (no.)	34,214	22,545	14,544	87,823
Map resolution (Å) FSC threshold	2.8	3.0	3.4	2.5
Map resolution range (Å)	0.143	0.143	0.143	0.143

Cytosolic ribosomes from 3mM Neo treated cells	Cytosolic ribosome, Non-rotated state, P/P-E/E	Cytosolic ribosome, Partially rotated state, eEF2, SERBP1, E/E	Cytosolic ribosome, Rotated state, A/P-P/E
EMDB	65416	65417	65418
Data collection and processing			
Magnification	96000x	96000x	96000x
Voltage (kV)	300	300	300
Electron exposure (e–/Å^2)	50	50	50
Defocus range (μm)	-1 to -2	-1 to -2	-1 to -2
Pixel size (Å)	0.81	0.81	0.81
Symmetry imposed	*C1*	*C1*	*C1*
Initial particle images (no.)	902,658	902,658	902,658
Final particle images (no.)	57,877	31,167	62,613
Map resolution (Å) FSC threshold	2.9	3.1	2.8
Map resolution range (Å)	0.143	0.143	0.143